

## Fringe Correction for STIS Near-IR Long-Slit Spectra using Contemporaneous Tungsten Flat Fields

Paul Goudfrooij<sup>1</sup> and Stefi A. Baum

*Space Telescope Science Institute, 3700 San Martin Drive, Baltimore, MD 21218*

Jeremy R. Walsh

*Space Telescope – European Coordinating Facility, Karl-Schwarzschild-Strasse 2,  
D-85748 Garching bei München, Germany*

**Abstract.** We report on the accuracy of fringe removal for STIS long-slit near-IR spectra using contemporaneous flats (taken during the course of science data collection). In case of point sources, we use tungsten flats taken through a small slit to mimic illumination by a point source. In case of extended sources, we use long-slit spectra of Jupiter’s moon Io as test cases. We find that in case of the G750L grating, fringe residuals can be reduced to below the 1% level, for both point sources and extended objects.

### 1. Introduction: Near-IR Fringing in CCD Spectra

Fringes in CCD observations arise from multiple reflections between the front and back surface of the CCD chip in case the distance between the surfaces is a small integer multiple of the wavelength of the incident monochromatic light from an external source. The small difference in path length gives rise to a series of bright and dark fringes. In effect the surfaces act as an interferometer. In the case of a CCD chip, the front and back surface are never exactly planar or parallel, which results in irregularly shaped fringes.

In the particular case of the STIS SiTE CCD, fringes are only appearing at the longer wavelengths ( $\lambda \geq 7000 \text{ \AA}$ ). If the light incident on any one resolution element is monochromatic (i.e., spectroscopy), the wavelength varies as a function of position along the dispersion direction. Therefore, the fringe pattern for any particular observing mode is a convolution of the contours of constant distance between the front and back surfaces and the wavelength of light incident on that particular part of the CCD. For medium-resolution data (i.e., the G750M grating), the wavelength changes slowly with position ( $\sim 0.5 \text{ \AA/pixel}$ ), so that the shape of the fringes is mostly dictated by the shape of the CCD, while for low-resolution data (G750L grating) the wavelength changes much more rapidly ( $\sim 5 \text{ \AA/pixel}$ ), so that the changing wavelength dictates the shape of the fringes.

Actual flat fields taken in dispersed light show peak-to-peak amplitudes growing to 25% and 32% at 9800  $\text{\AA}$  for the G750L and G750M gratings, respectively. Figs. 1 and 2 depict typical flat fields for the G750L and G750M gratings.

Rectification of the fringing pattern should be a tractable problem, because the behavior is entirely stable with time. However, small shifts in the wavelength mapping onto the detector, caused by grating wheel non-repeatability and thermal drifts on orbit, do cause the fringe pattern to shift from exposure to exposure. Therefore, for accurate fringe removal it is necessary to take contemporaneous spectral flats using the onboard tungsten lamps.

---

<sup>1</sup>Affiliated with the Astrophysics Division, Space Science Department, European Space Agency

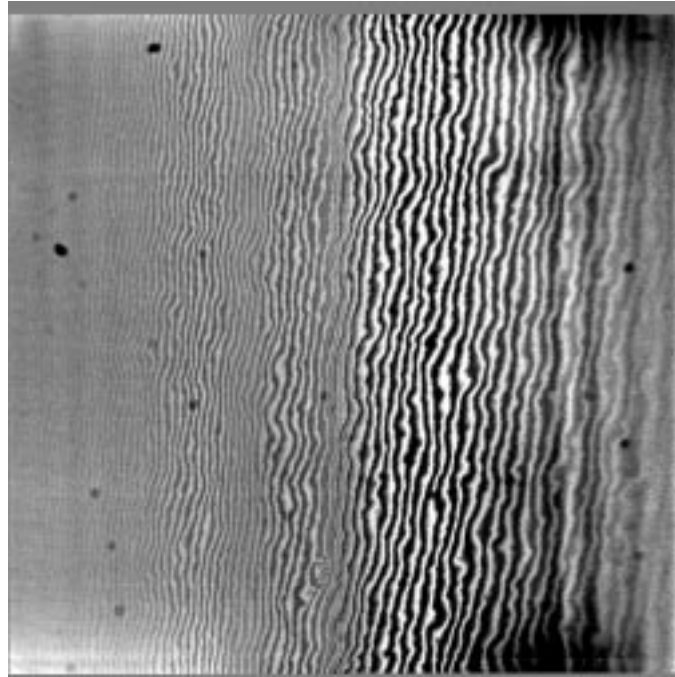


Figure 1. Grey-scale plot of normalized G750L flat field at a central wavelength of 8975 Å. Display cuts are  $\pm 10\%$ .

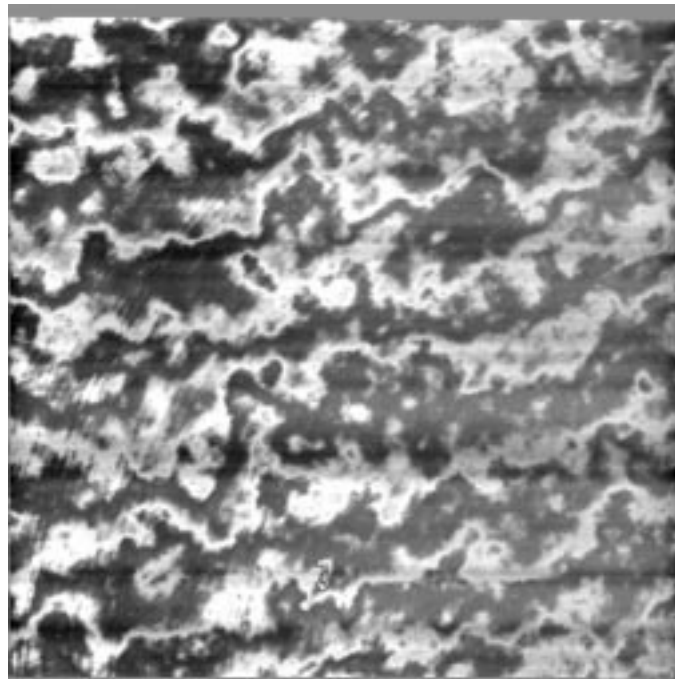


Figure 2. Grey-scale plot of normalized G750M flat field at a central wavelength of 9851 Å. Display cuts are  $\pm 20\%$ .

## 2. Fringe Correction for Extended Sources

To test the fringe correction for extended sources, we obtained long-slit spectra of Io (diameter is 1.15 arcsec) with the 52×0.2 slit and grating G750L (at 7751 Å) along with contemporaneous flats with the same set-up. Io was moved along the slit after each exposure, so that each set of data are corrected by different parts of the flat field. By sampling the intrinsically same region of Io from each individual exposure, any differences among the individual spectra must then be attributable to the flat field correction. We have then averaged the (three) different spectra together, after dividing by (i) no flat at all, (ii) the library (pre-flight) flat (which is used in the STIS pipeline reduction `calstis`), and (iii) the contemporaneous flat. The latter flat was produced by applying `calstis` without flatfield correction, and fitting a cubic spline through each line of the tungsten exposure using the `iraf.twodspec.longslit.response` routine.

Fig. 3 depicts the results of flatfielding the G750L spectra of Io using these three different methods. The residual RMS “noise” in channels 500 – 850 ( $\sim 7630 - 9340$  Å) is 0.9% using the contemporaneous flat, vs. 5.4% for the pre-flight flatfielded data.

## 3. Fringe Correction for Point Sources

Due to scattered light problems, flat field images taken with the standard long slit (52 arcsec long) do not mimic the illumination by a point source adequately without further reduction. One way to accomplish a correction for the influence of scattered light is to assume the amount of scattered light to be equal to the residual light under the fiducial occulting bars of the STIS spectrograph. After this correction for scattered light, long-slit flats are found to be able to reduce fringing to  $\sim 2-3\%$  (cf. Plait & Lindler 1997).

Another method of fringe correction for point sources is to use contemporaneous flats through a short slit which are typically used for echelle spectroscopy (i.e., the 0.2×0.06 or the 0.3×0.09 slit, depending upon which of the two is closer [in the dispersion direction] to the long-slit being used), which should mimic a point source much more accurately. To test the fringe correction for point sources, we used well-exposed spectra of the white dwarf GD 153 using the 52×2 slit and grating G750L (at 7751 Å), which is part of the regular CCD contamination/sensitivity monitor. An ACQ/PEAK peak-up was performed so that the star was very well centered in the slit. A pair of contemporaneous tungsten flats with the 0.3×0.09 slit was taken just before the star observation. Figs. 4 and 5 depict the G750L spectrum of GD 153 reduced with the pipeline (pre-flight) flat and with the contemporaneous flat, respectively. As mentioned above in Section 2, the contemporaneous flat was produced by applying `calstis` without flatfield correction, and fitting a cubic spline through each line of the tungsten exposure using the `response` routine. The residual RMS “noise” in channels 500 – 850 ( $\sim 7630 - 9340$  Å) is 0.95% using the contemporaneous flat, vs. 5.4% for the pre-flight flatfielded data.

## 4. Concluding Remarks

- Fringe removal from G750L spectra can be greatly improved using contemporaneous flat fields. Fringe residuals are approximately 1% in the cases analyzed so far. In the case of G750M spectra (not shown), the improvement is also clear but less dramatic, as expected since the fringing is mostly due to the shape of the CCD chip in that case.
- An STSDAS task for fringe removal using contemporaneous flats for STIS long-slit spectra will be implemented in the near future.
- As of the time of writing, the RPS2 interface for specifying contemporaneous flats is still under development, so they must be inserted by hand into the proposal during

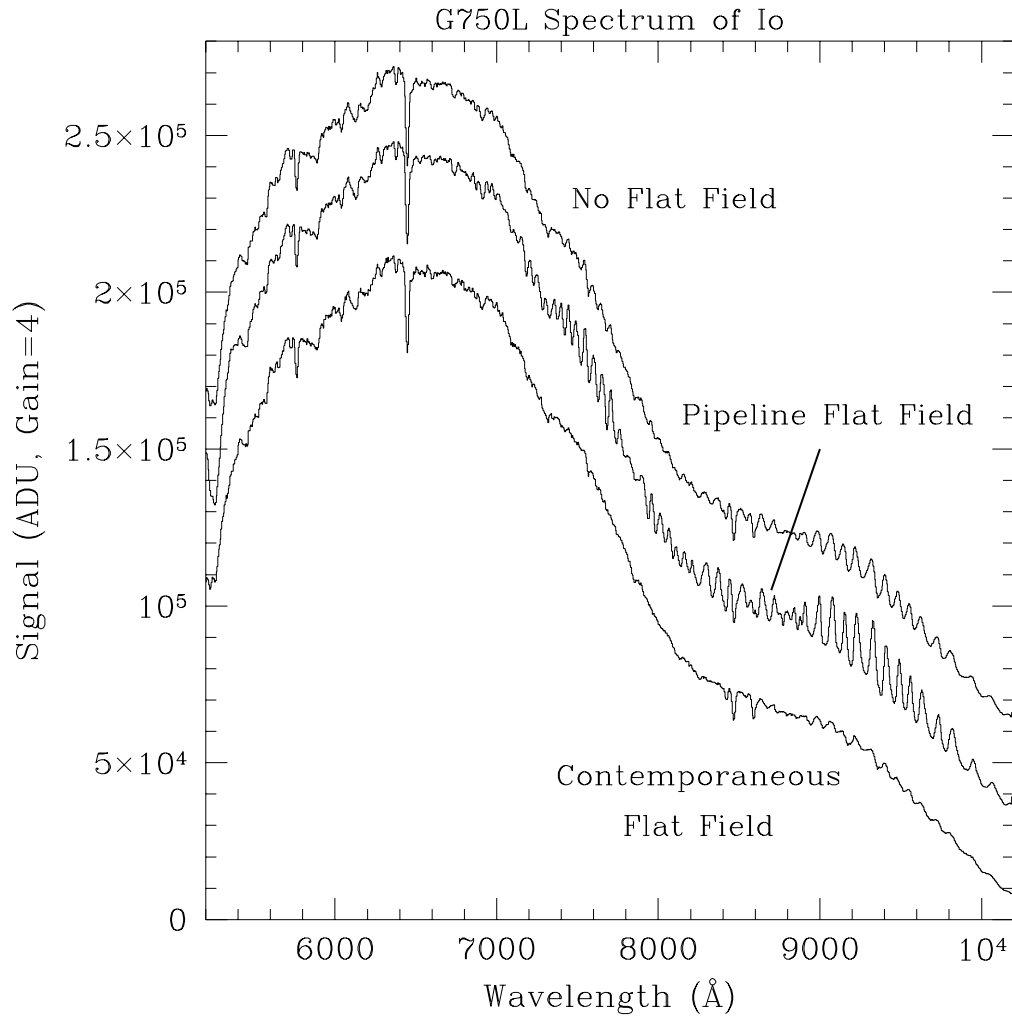


Figure 3. Comparison of G750L spectra of Jupiter's moon Io. The central wavelength is  $7751 \text{ \AA}$ , and the  $52 \times 0.2$  slit was used. (*i*, *top*) reduced without flat fielding, (*ii*, *middle*) flatfielded with the standard pipeline (pre-flight) flat, and (*iii*, *bottom*) flatfielded with a contemporaneous flat taken during the same orbit as the Io spectra, with the same observational setup. Notice the rather dramatic difference in fringe amplitude.

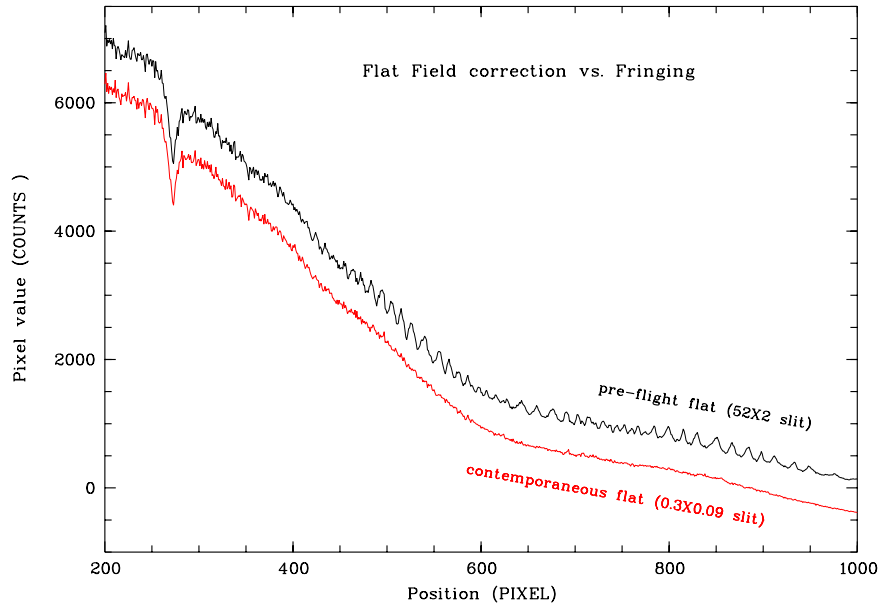


Figure 4. Comparison of two G750L spectra of white dwarf GD 153. The central wavelength was  $7751 \text{ \AA}$ , and the  $52 \times 2$  slit was used. (*i*, *top*) flatfielded with the standard pipeline (pre-flight) flat which was taken through the  $52 \times 0.1$  slit, and (*ii*, *bottom*) flatfielded with a contemporaneous flat taken during the same orbit as the Io spectra, taken through the  $0.3 \times 0.09$  slit, which is normally used for echelle observations. The latter spectrum has been shifted downward by an arbitrary amount for clarity reasons. Notice the rather dramatic difference in fringe amplitude.

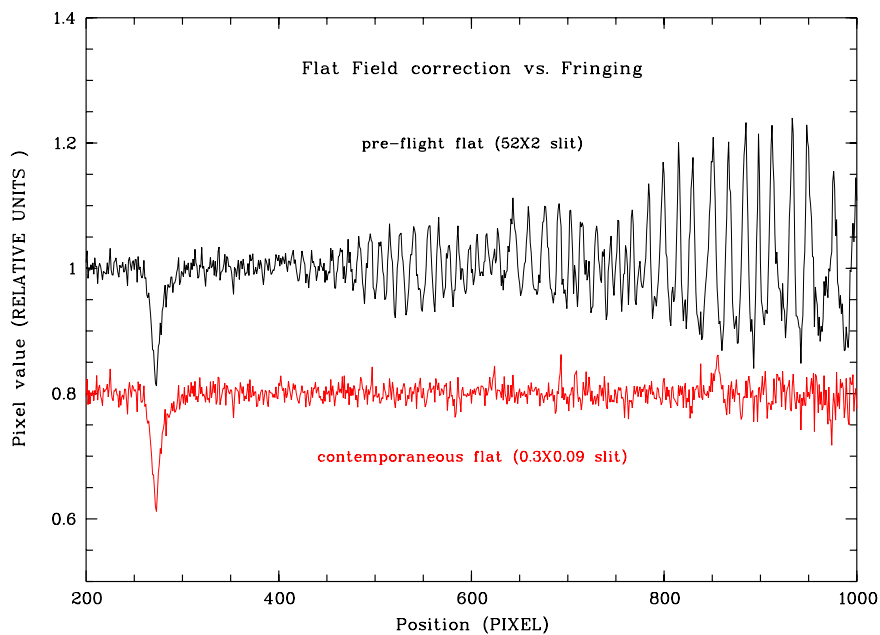


Figure 5. As Fig. 4, but divided by the stellar continuum to show the relative amplitude of the fringes.

phase-B preparation. Observers using G750L or G750M at wavelengths longer than 7000 Å should keep this in mind when finalizing their proposals.

#### **4.1. Possible Future Improvements**

- Fringe correction using a library of in-flight long-slit tungsten flat fields: As time goes by and the number of in-flight tungsten flat fields increases, it will be possible to build a library of long-slit flat field images in the different spectroscopic modes; one can envisage being able to query this library by e.g., the peak of the cross-correlation with a reference flat field for each particular mode, so that one could pick the best library flat for use with any particular long-slit spectrum.
- Fringe correction using White Dwarf Models: comparing observed white dwarf spectra with model atmospheres and building a library of flats from that. These may be quite useful for de-fringing spectra since they are typically of high S/N and no “point-source mimicking” is necessary. Note that in this case, the user will have to apply a shift along the dispersion to the “fringe flat” before de-fringing.

#### **References**

Plait, P., & Lindler, D., 1997, this volume.